Journal of Visualized Experiments

Hydrogen Charging of Aluminum using Friction in Water

--Manuscript Draft--

Article Type:	Methods Article - JoVE Produced Video
Manuscript Number:	JoVE60711R2
Full Title:	Hydrogen Charging of Aluminum using Friction in Water
Section/Category:	JoVE Engineering
Keywords:	Hydrogen; Aluminum; Friction in water; Hydrogen charging; Chemical reaction; Gas chromatography; Thermal desorption analysis; Hydrogen embrittlement
Corresponding Author:	Keitaro Horikawa Osaka University Toyonaka, 560-8531 JAPAN
Corresponding Author's Institution:	Osaka University
Corresponding Author E-Mail:	horikawa@me.es.osaka-u.ac.jp
Order of Authors:	Keitaro Horikawa
	Hidetoshi Kobayashi
Additional Information:	
Question	**Response**
Please indicate whether this article will be Standard Access or Open Access.	Standard Access (US$2,400)
Please indicate the **city, state/province, and country** where this article will be **filmed**. Please do not use abbreviations.	1-3 Machikaneyama, Toyonaka city, Osaka profecture, Japan

TITLE:

Hydrogen Charging of Aluminum using Friction in Water

AUTHORS AND AFFILIATIONS:
Keitaro Horikawa[1], **Hidetoshi Kobayashi**[1]
[1]Department of Mechanical Science and Bioengineering, Osaka University, Toyonaka, Osaka, Japan

Corresponding author:
Keitaro Horikawa (horikawa@me.es.osaka-u.ac.jp)

Email Addresses of Co-author:
Hidetoshi Kobayashi (hkoba@me.es.osaka-u.ac.jp)

KEYWORDS:
hydrogen, aluminum, friction in water, hydrogen charging, chemical reaction, gas chromatography, thermal desorption analysis, hydrogen embrittlement

SUMMARY:
In order to introduce high amounts of hydrogen in aluminum and aluminum alloys, a new method of hydrogen charging was developed, called the friction in water procedure.

ABSTRACT:
A new method of hydrogen charging of aluminum was developed by means of a friction in water (FW) procedure. This procedure can easily introduce high amounts of hydrogen into aluminum based on the chemical reaction between water and non-oxide coated aluminum.

INTRODUCTION:
In general, aluminum base alloys have higher resistance to environmental hydrogen embrittlement than steel. The high resistance to hydrogen embrittlement of aluminum alloys is due to oxide films on the alloy surface blocking hydrogen entry. To evaluate and compare the high embrittlement sensitivity between aluminum alloys, hydrogen charging is usually performed prior to mechanical testing[1-17]. However, it is known that hydrogen charging aluminum is not easy, even when utilizing hydrogen charging methods such as cathodic charging[15], slow strain rate deformation under humid air[16], or hydrogen plasma gas charging[17]. The difficulty of hydrogen charging aluminum alloys is also due to the oxide films on the aluminum alloy surface. We postulated that higher amounts of hydrogen could be introduced into aluminum alloys if we could remove the oxide film continuously in water. Thermodynamically[18], pure aluminum without oxide film reacts easily with water and generates hydrogen. Based on this, we have developed a new method of hydrogen charging of aluminum alloys based on the chemical reaction between water and non-oxide aluminum. This method is able to add high amounts of hydrogen into aluminum alloys in a simple way.

PROTOCOL:

1. Material preparation

1.1. Use 1 mm thick plates made of an aluminum-magnesium-silicon alloy containing 1 mass% Mg and 0.8 mass% Si (Al-Mg-Si).

1.2. Make test pieces from the Al-Mg-Si alloy plates having a gauge length of 10 mm and width of 5 mm.

1.3. Anneal the test pieces at 520 ˚C for 1 h using an air furnace. Quench in water as a solution heat treatment.

1.4. Anneal the test pieces at 175 ˚C for 18 h as a peak aging heat treatment (T6-temper).

1.5. Polish the surface of the test pieces using silicon carbide emery paper (#2000) without water.

1.6. Measure the weight of the polished specimens to a precision of 0.0001 g using an electric balance

1.7. Measure the thickness and width of the gauge part of the specimens to a precision of 0.001 mm using an optical comparator.

2. FW procedure (Figure 1)

2.1. Attach two Al-Mg-Si alloy specimens using glue to a triangular, prism-shaped stirrer made by a fluorocarbon polymer.

2.2. Prepare a cylinder glass container with an empty top as a reaction vessel.

2.3. Attach a round polishing paper made by silicon carbides, #2000 with a diameter of 10 mm, using double sided tape in the bottom inside of the container.

2.4. Place the triangular, prism-shaped stirrer with two specimens on the polishing paper at the bottom surface of the glass container.

2.5. Pour 100 mL of distilled water into the glass container from the top.

2.6. Cover the glass container with a round rubber piece with three holes (for a gas inlet, for a gas outlet, and for a pH probe at the top of the glass container).

2.7. Fill the glass container with high purity (99.999%) argon at a constant flow rate of 20 mL/min after closing the rubber cover.

2.8. Connect the gas outlet to a gas chromatograph (GC) with a semiconductor hydrogen sensor (detection limit: 5 ppb).

2.9. Wait until the gas in the container is replaced by argon.

2.10. Rotate the triangular, prism-shaped stirrer with two specimens on a magnetic stirrer with a constant rotating speed at room temperature.

2.11. Measure the hydrogen generation during the stirrer rotation using the GC, taking one measurement every 2 min.

2.12. Measure the pH of the water in the container during the stirrer rotation.

2.13. Remove the two specimens from the triangular, prism-shaped stirrer by immersion in acetone with an ultrasonic vibration for 5 min after the FW procedure.

2.14. Measure the weight and thickness of the specimens again after the FW procedure using the electric balance and an optical comparator, respectively.

3. Hydrogen absorption by the FW procedure

3.1. After the FW procedure, cut a specimen to a rectangular shape of 1 x 5 x 10 mm.

3.2. Place the specimen inside a quartz tube with a diameter of 10 mm connected to a GC with a semiconductor hydrogen sensor.

3.3. Flow high purity (99.999%) argon gas in a quartz tube with a constant flow rate of 20 mL/min.

3.4. Heat the quartz tube with the specimen using a tubular furnace at a constant heating rate, 200 ˚C/h.

3.5. Measure the thermal hydrogen desorption of the specimen after the FW procedure using the GC.

4. Material evaluation after the FW procedure

4.1. Carry out tensile tests (at least 3x, to ensure repeatability) in laboratory air with a crosshead speed of 2 mm/min using a specimen that has been treated by the FW procedure.

4.2. Measure the tensile properties (e.g., tensile strength, fracture strain) obtained from the stress-strain curve in the tensile test.

4.3. Observe the fracture behavior with a secondary electron microscope (SEM) after the tensile test.

REPRESENTATIVE RESULTS:

Hydrogen generation/absorption by the FW procedure

Figure 2 shows the hydrogen generation behavior during the FW procedure of Al-Mg-Si alloys containing different amounts of iron from 0.1 mass % to 0.7 mass %. The specimen continuously emitted a high amount of hydrogen when the stirrer started to rotate. This suggests that hydrogen was generated by a chemical reaction caused by the friction between the alloy surface and water. In addition, the pH value of the water during the FW procedure increased slightly from 6.5–7.5 as shown in **Figure 3**. The change in pH by the FW procedure would not affect the corrosive reaction based on the electrochemical diagram proposed by Pourbaix[19].

Figure 4 shows the TDA results in samples with and without hydrogen charging by the FW procedure of the Al-Mg-Si alloys. Regardless of the alloy composition of the specimen, the total hydrogen concentration after the FW procedure increased compared to the original uncharged state. In all samples after the FW procedure, hydrogen evolution occurred at above 400 °C. A small peak of hydrogen evolution was also visible around 300 °C–400 °C in the hydrogen-charged samples. The hydrogen evolution peak around 300 °C–400 °C would be related to hydrogen trapping by lattice defects, such as dislocations and grain boundaries[20,21]. The hydrogen concentration calculated by integrating the hydrogen release rate and the temperature from 25 ˚C–625 ˚C is shown in **Figure 5**. It is obvious that the hydrogen concentration after the FW procedure increased about 4x from the original state.

Figure 6 shows the comparison of hydrogen concentration between the FW procedure and the hydrogen charging by pre-strain of 0.1 under a humid air atmosphere with a relative humidity of 90% in a 0.1% iron specimen. It is also clear that the hydrogen charging by the FW procedure allowed the introduction of large amounts of hydrogen compared to the charging by pre-strain under humid air.

Mechanical performance after the FW procedure

Figure 7 shows the tensile test results of both the hydrogen-uncharged samples and hydrogen-charged samples. A decrease in ductility was observed in the Al-Mg-Si alloy with 0.1% iron just after the FW procedure. This indicates that the Al-Mg-Si alloy with 0.1% iron shows hydrogen embrittlement caused by the high amount of hydrogen charging by the FW procedure.

The fracture morphology of the Al-Mg-Si alloy with 0.1% iron changed to a grain boundary fracture after the hydrogen charging by the FW procedure, particularly adjacent to the hydrogen entry side as shown in **Figure 8**. This indicates that hydrogen atoms introduced by the FW procedure enhance the decohesion of grain boundaries, which leads to hydrogen embrittlement, in the Al-Mg-Si alloy with 0.1% iron.

FIGURE LEGENDS:

Figure 1: Schematic of the apparatus used in the FW procedure.

Figure 2: Hydrogen generation during the FW procedure. (**A**) 0.1% Fe, (**B**) 0.2% Fe, (**C**) 0.7% Fe.

Figure 3: Change of pH during the FW procedure. (**A**) 0.1% Fe, (**B**) 0.2% Fe, (**C**) 0.7% Fe.

Figure 4: Thermal hydrogen desorption analysis of Al-Mg-Si alloys with iron. (**A**) 0.1 Fe, (**B**) 0.2% Fe, (**C**) 0.7%Fe.

Figure 5: Hydrogen concentration with and without the FW procedure. (**A**) 0.1% Fe, (**B**) 0.2% Fe, (**C**) 0.7% Fe.

Figure 6: **Comparison of thermal desorption analysis and hydrogen concentration of Al-Mg-Si alloys with 0.1% Fe in different hydrogen charging conditions.**

Figure 7: Stress-strain curves of the Al-Mg-Si alloy with 0.1% Fe, **before and just after the FW procedure.**

Figure 8: **Fracture surfaces of an Al-Mg-Si alloy with 0.1% Fe.** (**A**) Before and (**B**) after the FW procedure, adjacent to the hydrogen entry side.

DISCUSSION:

One important aspect of the FW procedure is the attachment of the two specimens to the magnetic stirrer. Because the center of the stirrer bar becomes the non-friction zone, it is best to avoid the attachment of the specimens at the center of the stirrer bar.

Control of the rotation speed of the stirrer bar is also important. When the speed is more than 240 rpm, it becomes difficult to maintain the reaction vessel on the stage of the magnetic stirrer. When the FW procedure is carried out at high speed, fixing the reaction vessel to the stage of the magnetic stirrer is needed.

Because the hydrogen charging by the FW procedure is based on the chemical reaction between water and a non-oxide coated aluminum surface, this is a simple method when compared to conventional hydrogen charging methods, such as cathodic charging[15], pre-strain under a humid air atmosphere[16]. A theoretical volume of generated hydrogen is calculated based on the change of weight in the sample before and after the FW procedure. Also, the FW procedure can introduce high amounts of hydrogen into aluminum. However, when the time of the FW procedure is longer, the pH value of water increases. When the pH value of water becomes >10, a corrosive reaction between aluminum and water may happen[16]. To prevent the corrosive reaction of the specimen, the time of the FW procedure should be limited so the pH value of the water solution ranges from 4–10.

In the FW procedure, the hydrogen charging is applicable basically to the plate shaped aluminum and aluminum alloys. The hydrogen charging in the FW procedure is based on hydrogen entry from one surface of the plate specimen.

ACKNOWLEDGMENTS:

This work was financially supported in part by The Light Metal Educational Foundation, Inc., Osaka, Japan

DISCLOSURES:

The authors have nothing to disclose.

REFERENCES:

1. Horikawa, K., Matsubara, T., Kobayashi, H. Hydrogen charging of Al-Mg-Si-based alloys by friction in water and its effect on tensile properties. *Materials Science and Engineering A*. **764**, 138199 (2019).
2. Horikawa, K. Current research trends in aluminum alloys for a high-pressure hydrogen gas container. *Journal of Japan Institute of Light Metals*. **60**, 542–547 (2010).
3. Kuramoto, S., Hsieh, M.-C., Kanno, M. Environmental embrittlement of Al-Mg-Si base alloys deformed at low strain rates in laboratory air. *Journal of Japan Institute of Light Metals*. **52**, 250–255 (2002).
4. Horikawa, K., Yoshida, K. Visualization of Hydrogen in Tensile-Deformed Al-5%Mg Alloy by means of Hydrogen Microprint Technique with EBSP Analysis. *Materials Transactions*. **45**, 315–318 (2004).
5. Ueda, K., Horikawa, K., Kanno, M. Suppression of high temperature embrittlement of Al-5%Mg alloys containing a trace of sodium caused by antimony addition. *Scripta Materialia*. **37**, 1105-1110 (1996).
6. Horikawa, K., Ando, N., Kobayashi, H., Urushihara, W. Visualization of hydrogen gas evolution during deformation and fracture in SCM 440 steel with different tempering conditions. *Materials Science and Engineering A*. **534**, 495–503 (2012).
7. Horikawa, K., Yamada, H., Kobayashi, H. Effect of strain rate on hydrogen gas evolution behavior during tensile deformation in 6061 and 7075 aluminum alloys. *Journal of Japan Institute of Light Metals*. **62**, 306-312 (2012).
8. Horikawa, K., Okada, H., Kobayashi, H., Urushihara, W. Visualization of diffusive hydrogen in low alloy steel by means of hydrogen microprint technique at elevated temperatures. *Materials Transactions*. **50**, 759-764 (2009).
9. Horikawa, K., Okada, H., Kobayashi, H., Urushihara, W. Visualization of hydrogen during fatigue fracture in an Al-Mg-Si alloy. *Journal of Japan Institute of Light Metals*. **56**, 210-213 (2006).
10. Horikawa, K., Okada, H., Kobayashi, H., Urushihara, W. Visualization of hydrogen distribution in tensile-deformed Al-5%Mg alloy investigated by means of hydrogen microprint technique with EBSP. *Journal of the Japan Institute of Metals*. **68**, 1043-1046 (2004).
11. Yamada, H., Tsurudome, M., Miura, N., Horikawa, K., Ogasawara, N. Ductility loss of 7075 aluminum alloys affected by interaction of hydrogen, fatigue deformation, and strain rate. *Materials Science and Engineering A*. **642**, 194-203 (2015).
12. Toda, H. et al. Effects of hydrogen micro pores on mechanical properties in a 2024 aluminum alloys. *Materials Transactions*. **54**, 2195-2201 (2013).
13. Yamada, H., Horikawa, K., Matsumoto, T., Kobayashi, H., Ogasawara, N. Hydrogen

evolution behavior of tensile deformation process in 6061 and 7075 aluminum alloys. *Journal of Japan Institute of Light Metals*. **61**, 297-302 (2011).
14. Horikawa, K., Kobayashi, H. Hydrogen absorption of pure aluminum by friction of the surface in water and its effect on tensile properties. *Journal of the Japan Institute of Metals*. **84**, in press (2020).
15. Suzuki, H., Kobayashi, D., Hanada, N., Takai, K., Hagihara, Y. Existing state of hydrogen in electrochemically charged commercial-purity aluminum and its effects on tensile properties. *Materials Transactions*. **52**, 1741-1747 (2011).
16. Horikawa, K., Hokazono, S., Kobayashi, H. Synchronized monitoring between hydrogen gas release and progress of atmospheric hydrogen embrittlement in 7075 aluminum alloy. *Journal of Japan Institute of Light Metals*. **66**, 77–83 (2016).
17. Manaka, T., Aoki, M., Itoh, G. Thermal desorption spectroscopy study on the hydrogen behavior in a plasma-charged aluminum. *Materials Science Forum*. **879**, 1220-1225 (2016).
18. Ellingham, H. J. T. Reducibility of oxides and sulphides in metallurgical processes. *Journal of the Society of Chemical Industry*. **63**, 125-133 (1944).
19. Pourbaix, M. *Atlas of electrochemical equilibria in aqueous solutions*, 1st ed. Pergamon Press, New York. p. 168–176 (1966).
20. Young Jr., G. A., Scully, J. R. The diffusion and trapping of hydrogen in high purity aluminum. *Acta Materialia*. **46**, 6337–6349 (1998).
21. Smith, S. W., Scully, J. R. The identification of hydrogen trapping states in an Al-Li-Cu-Zr alloy using thermal desorption spectroscopy. *Metallurgical and Materials Transactions A*. **31**, 179-193 (2000).

Figure 1

Click here to access/download;Figure;Fig.1.pdf

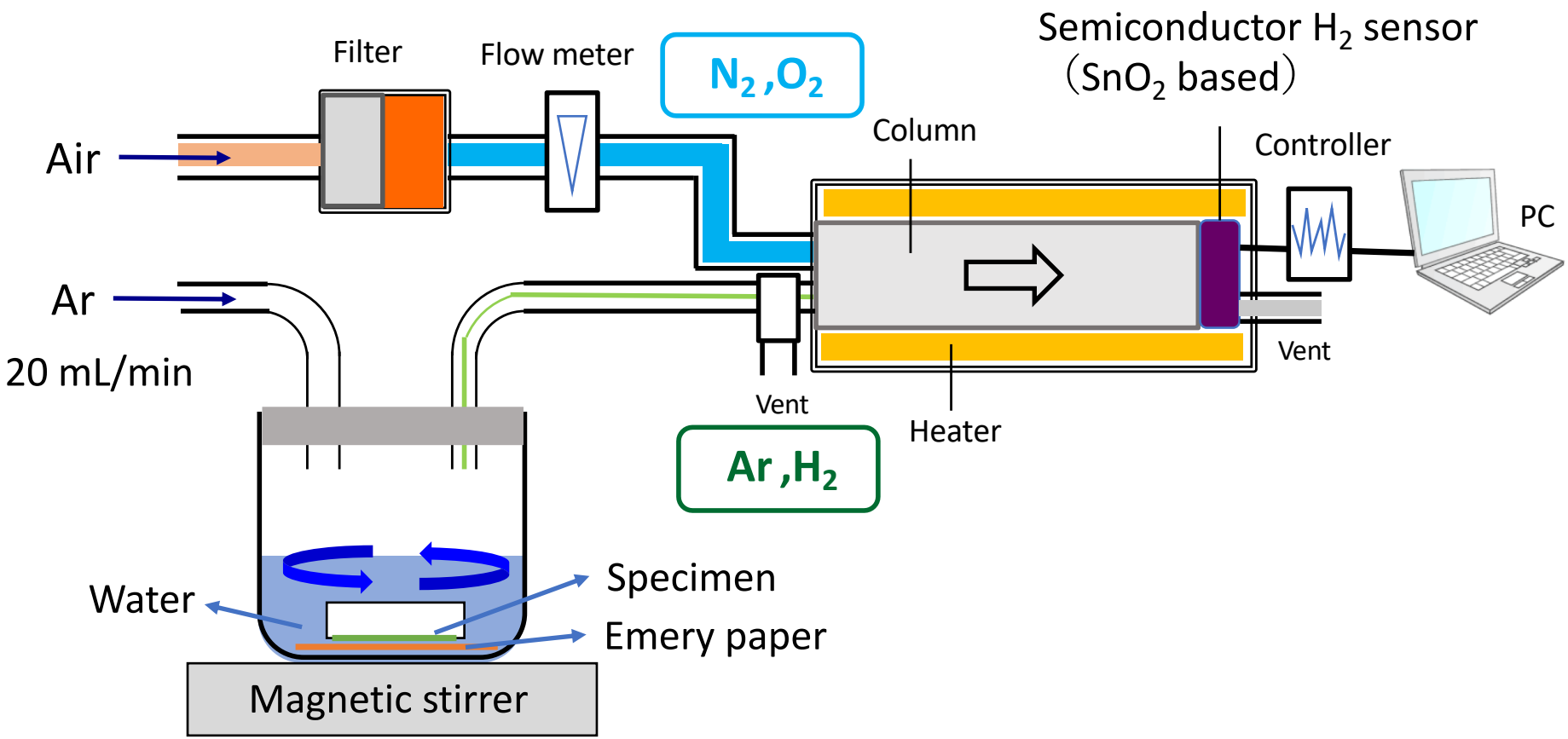

Figure 2

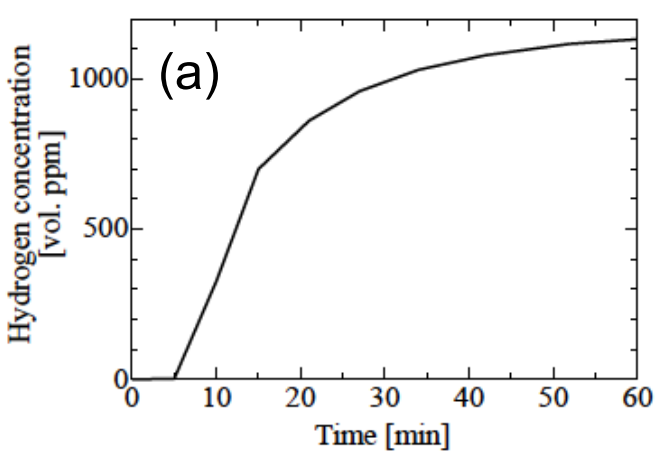

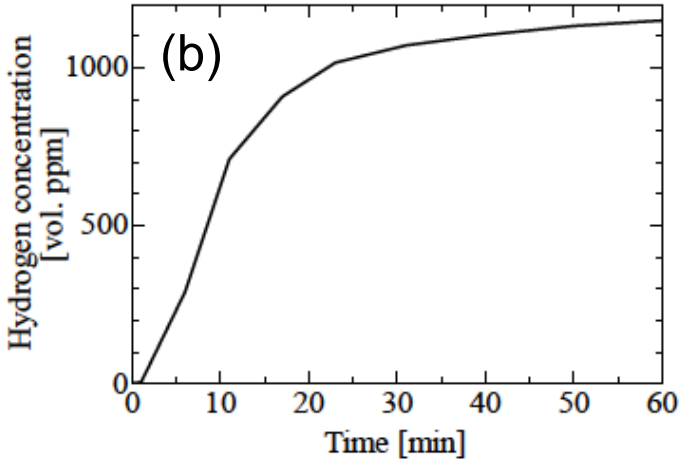

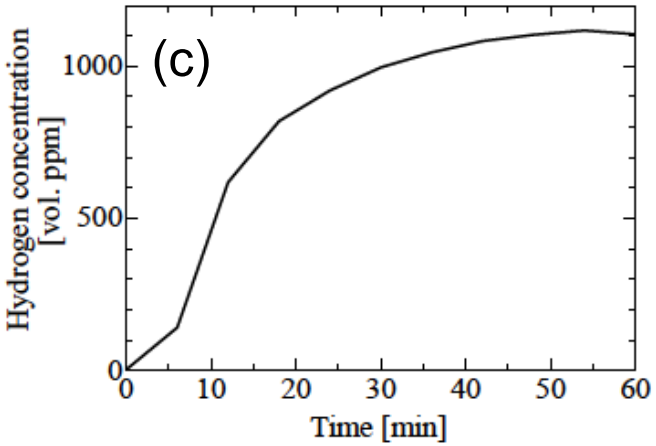

Figure 3

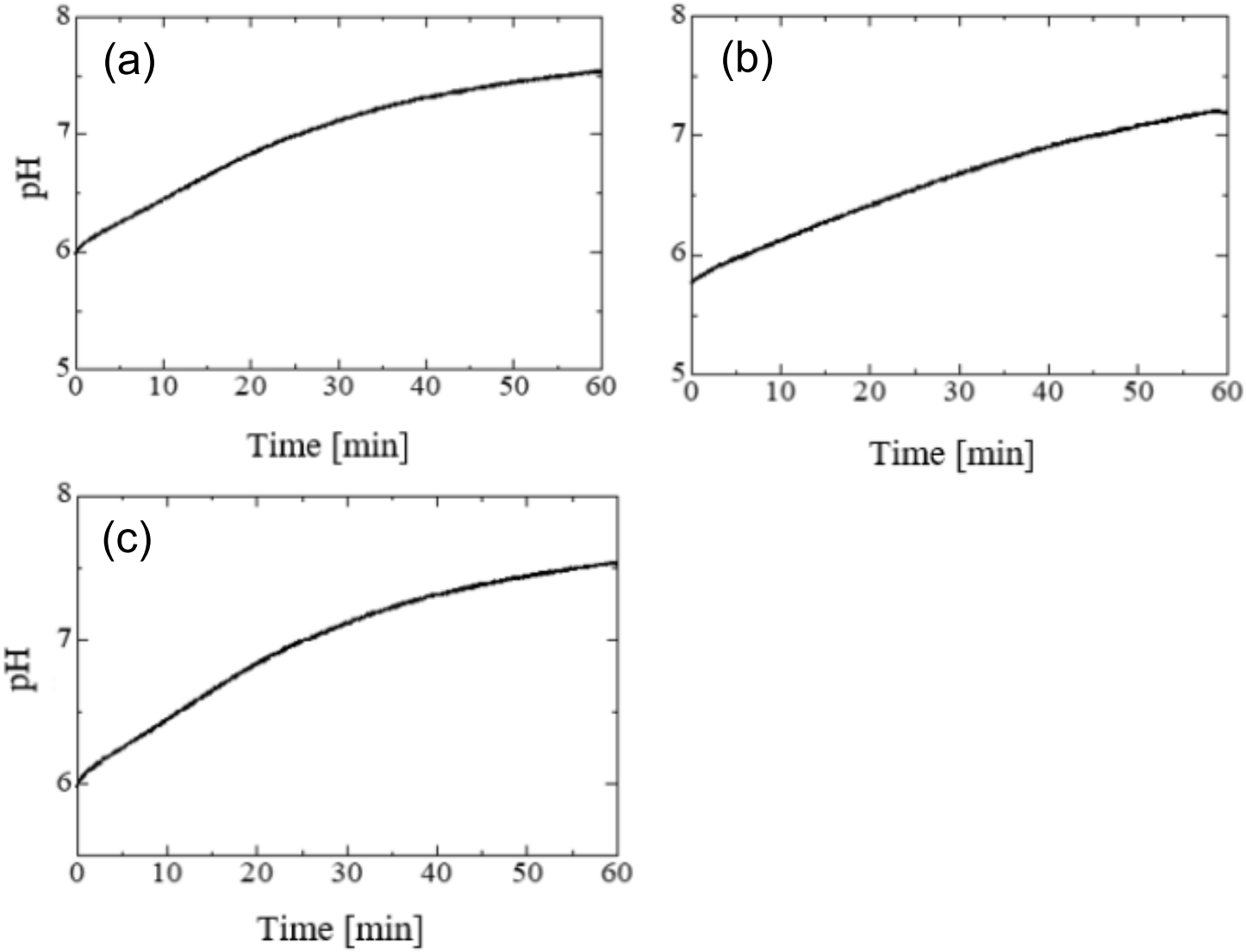

Figure 4

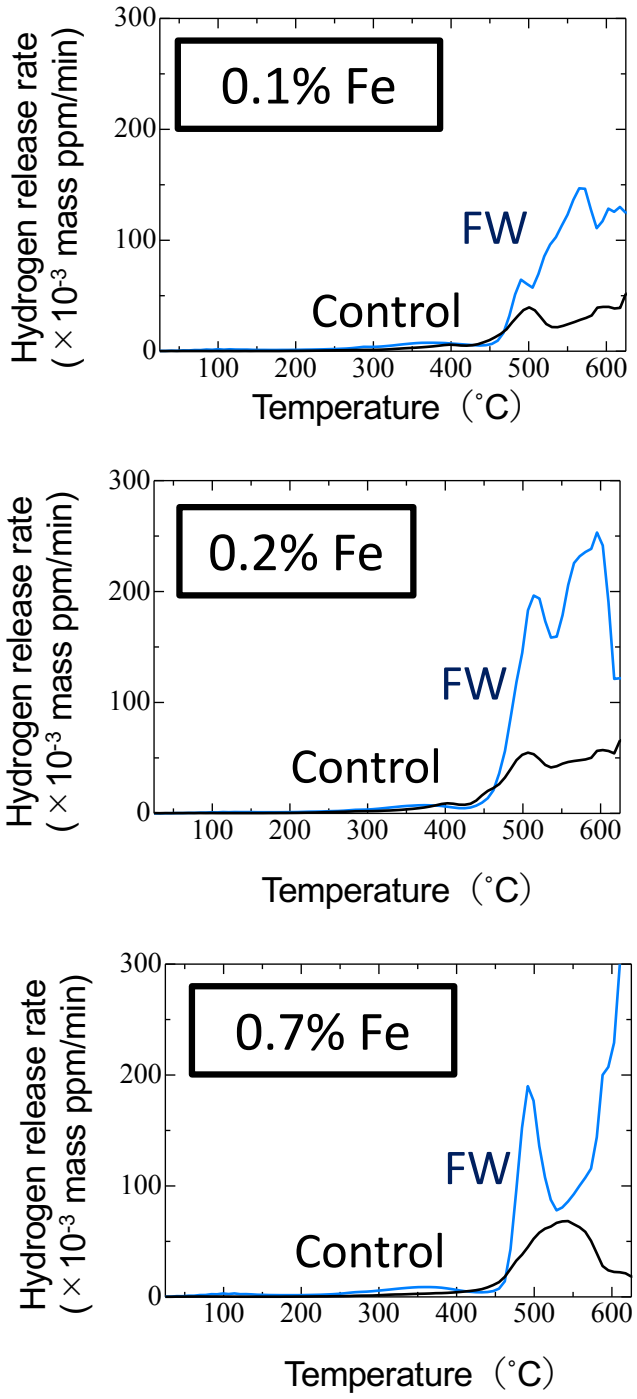

Figure 5

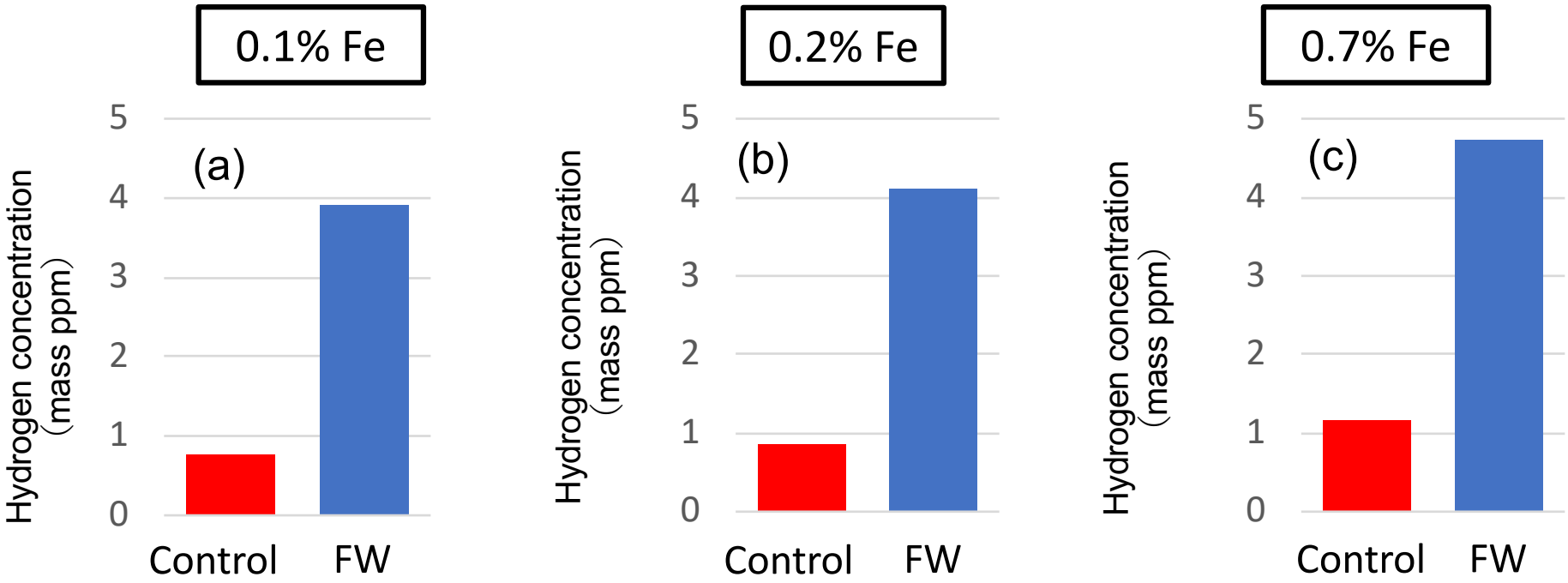

Figure 6

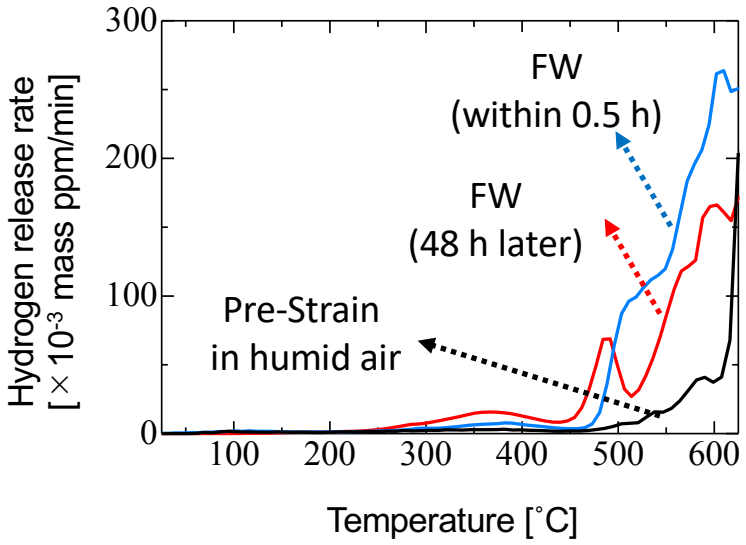

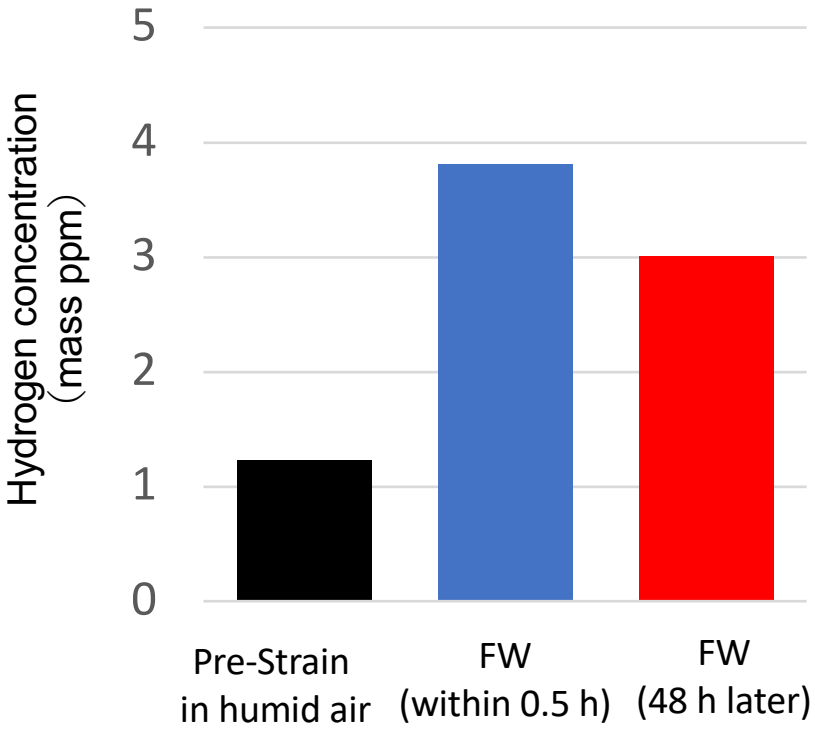

Figure 7

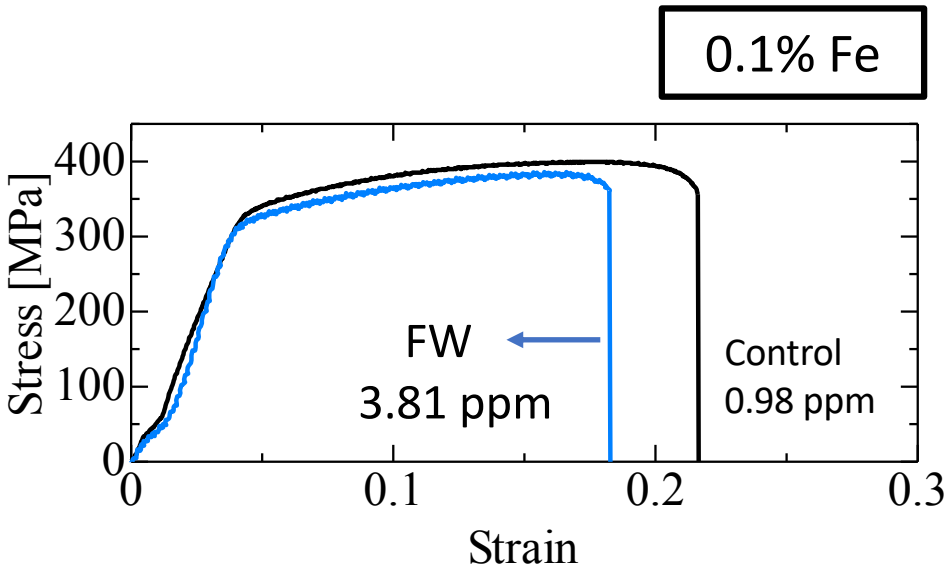

Figure 8

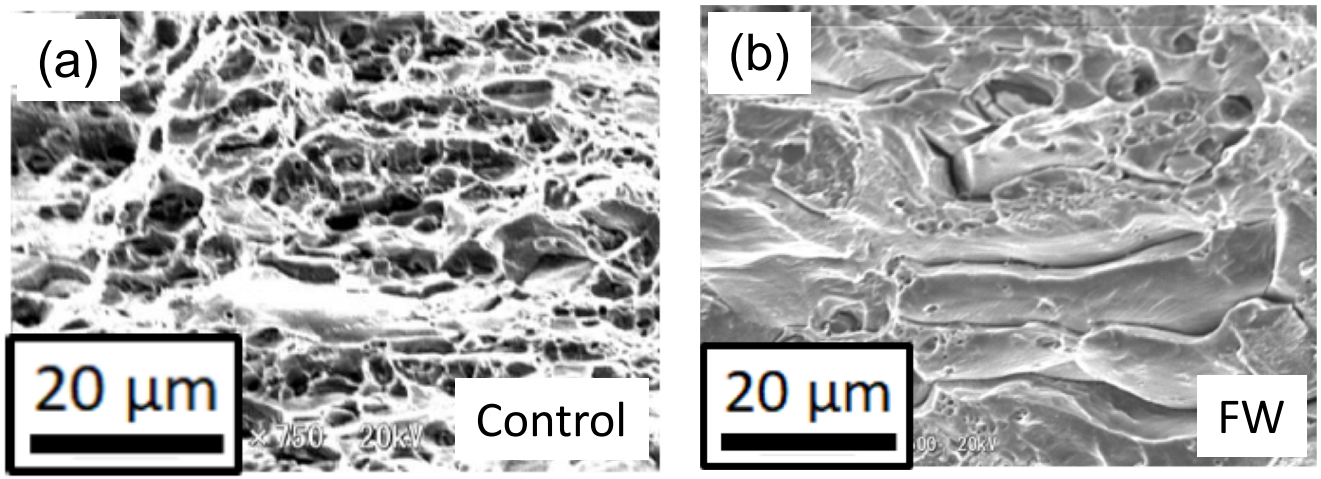

Table of Materials

Click here to access/download;Table of Materials;JoVE_Materials.xlsx

Name of Material/ Equipment	Company	Catalog Number
Air furnace	GC	QC-1
Aluminum alloy plates	Kobe Steel	
Electric balance	A&D	HR-200
Glass container		
Magnetic stirrer	CORNING	PC-410D
Optical Comparator	NIKON	V-12B
pH meter	Sato Tech	PH-230SDJ
Quartz tube		
Rotary polishing machine	IMT	IM-P2
Secondary electrom microscope	JOEL	JSM-5310LV
Sensor gas chromatograph	FIS Inc.	SGHA
Silicon carbide emery paper	IMT	531SR
Tensile testing machine	Toshin Kogyo	SERT-5000-C
Tubular furnace	Honma Riken	

Comments/Description
Al/1.0 mass% Mg/0.8mass% Si
Custom made
Custom made
Custom made

7 Nov. 2019

Editor
JOVE

Dear Editor:

I wish to resubmit a revised paper for publication in *JOVE* titled "A method of hyderogen charging in aluminum by means of friction in water process" The paper was coauthored by Hidetoshi Kobayashi.

According to the comments, we revised the manuscript and the figures as follows;

1

a. 1.1 We added the information of test material in the Table of Material.
b. 1.7/2.13 The name of universal projector is changed into "optical comparator". We added the information how to use it.
c. 3.5 We added the information how to perform the thermal desorption analysis.
d. 4. We explained that each properties are obtained from the stress-strain curves in the test.

2.

Except for the first appearance of Al-1mass%Mg-0.8mass%Si, we change the name of the alloy into Al-Mg-Si alloy.

3.

a-d

We modified the mistakes in the Figure as advised.

I hope that these corrections and revisions will be satisfactory for editorial comments.

Sincerely,

Keitaro Horikawa
Department of Mechanical Science and Bioengineering,
School of Engineering Science, Osaka University
1–3 Machikaneyama, Toyanaka 560-8531, Japan
+81-6-6850-6201
horikawa@me.es-osaka-u.ac.jp